

# Implementation of Tomlinson Harashima Precoder (THP) in Cloud Radio Access Networks (CRANs)

Neagin N S

A Thesis Submitted to  
Indian Institute of Technology Hyderabad  
In Partial Fulfillment of the Requirements for  
The Degree of Master of Technology



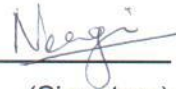
भारतीय प्रौद्योगिकी संस्थान हैदराबाद  
Indian Institute of Technology Hyderabad

Department of Electrical Engineering

June 2015

## Declaration

I declare that this written submission represents my ideas in my own words, and where others' ideas or words have been included, I have adequately cited and referenced the original sources. I also declare that I have adhered to all principles of academic honesty and integrity and have not misrepresented or fabricated or falsified any idea/data/fact/source in my submission. I understand that any violation of the above will be a cause for disciplinary action by the Institute and can also evoke penal action from the sources that have thus not been properly cited, or from whom proper permission has not been taken when needed.



---

(Signature)

---

(Neagin N S)

---

(EE13M1005)

## Approval Sheet

This thesis entitled Implementation of THP precoder in CRANs by Neagin N S is approved for the degree of Master of Technology/ Doctor of Philosophy from IIT Hyderabad.



\_\_\_\_\_  
-Name and affiliation-

Examiner



\_\_\_\_\_  
-Name and affiliation-

Examiner

(KIRAN KUCHI)

  
\_\_\_\_\_  
-Name and affiliation-

Adviser

\_\_\_\_\_  
-Name and affiliation-

Co-Adviser

  
\_\_\_\_\_  
-Name and affiliation-

Chairman

## Acknowledgements

I am using this opportunity to express my gratitude to everyone who supported me throughout the course of this M.Tech project. I am thankful for their aspiring guidance, invaluable constructive criticism and friendly advice during the project work. I am sincerely grateful to them for sharing their truthful and illuminating views on a number of issues related to the project.

I express my warm thanks to Dr. Kiran Kuchi and Mr. Sreejith T V for their support and guidance at IITH.

I would also like to thank my colleagues Mr. Harsha, Mr. Sibgath Ali, Mr. Sreekanth and Mr. Abhishek and all the people who provided me with the facilities being required and conducive conditions for my M. Tech project.

# Dedication

*Dedicated to my family and teachers*

## Abstract

The evolution of cellular communication networks from 1G through 4G has resulted in a steady increase in the allowable rates for users (UEs). However, other cell interference (OCI) still remains the performance limiting factor. OCI is the interference from signals received from other cells. Mitigation of OCI using interference cancellation strategies results in improvement of allowable rates. This can be achieved by Cloud radio access networks (C-RANs), which is also labeled as network multiple-input-multiple-output (MIMO) centralized precoding architecture in literature.

Precoders in CRANs are designed to presubtract the known interference at the transmitter. It basically exploits transmit diversity by weighting information stream, i.e. the transmitter send the coded information to the receiver in accordance with the pre-knowledge of the channel. A nonlinear precoder named THP precoder is implemented in my project work.

# Contents

Declaration . . . . .	ii
Approval Sheet . . . . .	iii
Acknowledgements . . . . .	iv
Abstract . . . . .	vi
<b>Nomenclature</b>	<b>vii</b>
<b>1 Introduction</b>	<b>1</b>
<b>2 CRANs</b>	<b>3</b>
2.1 System layout . . . . .	3
2.2 Voronoi diagram . . . . .	3
<b>3 Precoders</b>	<b>5</b>
3.1 Channel and pathloss model . . . . .	5
3.2 Received signal vector . . . . .	6
3.3 THP Precoders . . . . .	6
3.3.1 Modulo Operation . . . . .	7
3.3.2 Transmitter operation . . . . .	7
3.3.3 Receiver operation . . . . .	9
3.4 THP implementation for 6x6 cloud . . . . .	10
3.4.1 Psuedo code for THP implementation in Matlab . . . . .	10
<b>4 Channel Estimation</b>	<b>12</b>
4.1 Least Square (LS) . . . . .	13
<b>5 Simulation Results</b>	<b>15</b>
<b>6 CRAN prototype implementation</b>	<b>16</b>
6.1 LTE Testbed . . . . .	17
6.1.1 Hardware . . . . .	17
6.1.2 Cloud Implementation . . . . .	17

# List of Figures

2.1	Voronoi diagram . . . . .	4
3.1	Transmitter schematic . . . . .	7
3.2	Receiver Schematic . . . . .	9
4.1	Subframe structure for BS 1 and BS 2 . . . . .	12
4.2	Subframe structure for BS 3 and BS 4 . . . . .	13
4.3	Subframe structure for BS 5 and BS 6 . . . . .	13
4.4	Different channels in a resource block . . . . .	14
5.1	BER VS SNR plot . . . . .	15
6.1	Table showing performance improvement for THP precoding of a resource element and LQ decomposition of the particular channel using different optimization schemes in CCS studio . . . . .	16
6.2	LTE Testbed . . . . .	17



# Chapter 1

## Introduction

The use of mobile communication networks has increased significantly in the past decades, in terms of complexity of applications, their required capacities, and heterogeneity of device types. So far, this trend has always been met by significant technological advancements and will continue to increase. The evolution of cellular communication networks from 1G through 4G has resulted in a steady increase in the allowable rates for users (UEs). However, other cell interference (OCI) still remains the performance limiting factor. OCI is the interference from signals received from other cells. Mitigation of OCI using interference cancellation strategies results in improvement of allowable rates. This can be achieved by Cloud radio access networks (C-RANs), which is also labeled as network multiple-input-multiple-output (MIMO) centralized precoding architecture in literature.

C-RANs have been recognized as a promising architecture for mobile operators to simultaneously maintain profitability and provide better services. The key idea of a C-RAN at the physical layer is to coordinate spatially separated base stations (BSs), such that a distributed antenna array is formed to help user transmissions. The baseband processing is done at the cloud, while the waveforms are exchanged between BSs and cloud through fiber. The function of the BS mainly involves carrier power amplification and transmission through an antenna. This type of BS with reduced functionality is referred to as a remote radio head-end (RRH). Use of low power RRHs generally reduces the size and cost significantly compared to conventional BSs. Furthermore, availability of baseband signals at the cloud enables interference suppression techniques to be used both in the downlink and the uplink. In addition, cloud facilitates traffic load balancing through joint scheduling among the RRHs [5]. Accurately evaluating the gains of coordination, however, is contingent upon using a network topology that models realistic cellular deployments.

We model the base stations' locations as a Poisson point process instead of traditional hexagonal grid model to provide a better analytical assessment of the performance of coordination. Since interference coordination is only feasible within clusters of limited size, we consider a random clustering process where cluster stations are located according to a random point process and groups of base stations associated with the same cluster coordinate [2].

Several linear and nonlinear precoding techniques have been used to mitigate OCI effects in wireless communication networks. Among them, Dirty Paper Coding (DPC) is the most effective one. DPC is practically not realizable because of complexity. So a system close to DPC and also

practically realizable is needed. THP has been shown to almost achieve the capacity of DPC with the advantage of a realizable transceiver architecture. The implementation details of THP has been included in this report.

# Chapter 2

## CRANs

In a cloud radio network, a group of near by base-stations (BSs) function in cooperation to cancel the interference due to each other. In the downlink, the cloud, which is a collection of multiple BSs, serves a group of users equipments (UEs) simultaneously with multiple streams. These streams are appropriately precoded, so that interference-free decoding is possible at the receiver end. In the uplink, the cloud receives multiple streams from each UE, a stream corresponding to each point to point channel between a BS and a UE. These streams are jointly decoded at the cloud to nullify interference effects. Those BSs with reduced functionality are called RRHs (Remote Radio Head ends). The locations of BSs and UEs are assumed to follow Poisson point process (PPP). Poisson point process is a particular kind of random process by which a set of isolated points are scattered about a line or a plane or a three-dimensional space or any of various other sorts of spaces. Often the term Poisson process is used to mean a Poisson point process in which the space in which isolated points are randomly scattered is a line, which in many applications represents time.

### 2.1 System layout

In the proposed system model, the locations of the BSs follow a uniform PPP(Poisson Point Process)  $\phi_b$  with an intensity  $\lambda_b$  BSs per unit area and the UEs follow another independent uniform PPP  $\phi_u$  with an intensity  $\lambda_u$  in Euclidean space. We follow the following simulation procedure. Consider a rectangular grid of area  $A$ . In each iteration of the program, we generated Poisson distributed variable  $k$  with intensity  $A\lambda_b$  for BSs and Poisson distributed variable  $l$  with intensity  $A\lambda_u$  for the UEs. Then  $k$  BSs and  $l$  UEs are distributed in the chosen area  $A$ . Each UE is associated with a primary BS which is the geographically closest BS to itself and all other BSs.

### 2.2 Voronoi diagram

In mathematics, a Voronoi diagram is a partitioning of a plane into regions based on distance to points in a specific subset of the plane. That set of points (called seeds, sites, or generators) is specified beforehand, and for each seed there is a corresponding region consisting of all points closer to that seed than to any other. These regions are called Voronoi cells. Voronoi diagram showing the distribution of BS and UE is shown in figure 2.1. Each Voronoi cell contains a BS and a number of

UEs. Thus each BS can have more than one UE associated with it (based on Euclidian distance). Basically, Voronoi cell consists of all points whose distance to a BS in that cell is less than or equal to the distance to other BSs. Each BS randomly selects one among the UEs in its voronoi region.

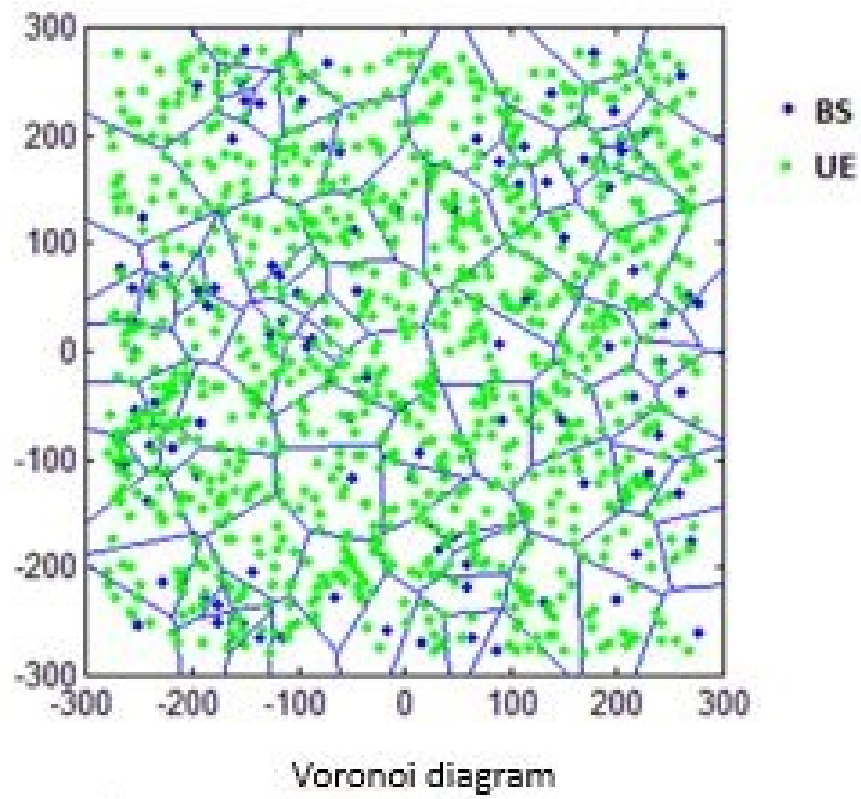


Figure 2.1: Voronoi diagram

# Chapter 3

## Precoders

Precoder presubtracts the known interference at the transmitter. It basically exploits transmit diversity by weighting information stream, i.e. the transmitter send the coded information to the receiver in accordance with the pre-knowledge of the channel. The receiver is a simple detector, such as a matched filter, and does not have to know the channel side information. This technique will reduce the corrupted effect of the communication channel.

In MIMO systems, precoding algorithms can be sub-divided into linear and nonlinear precoding types. The capacity achieving algorithms are nonlinear, but linear precoding approaches usually achieve reasonable performance with much lower complexity. Linear precoding strategies include maximum ratio transmission (MRT), zero-forcing (ZF) precoding, and transmit Wiener precoding. There are also precoding strategies tailored for low-rate feedback of channel state information, for example random beamforming and Tomlinson-Harashima precoding(THP). Nonlinear precoding is designed based on the concept of dirty paper coding (DPC), which shows that any known interference at the transmitter can be subtracted without the penalty of radio resources if the optimal precoding scheme can be applied on the transmit signal. DPC is practically not realizable because of complexity, So a system close to DPC and also practically realizable is needed, and THP is the one which can be used. In THP, transmit power is more compared to DPC. But the power increase is less for large constellations. So we usually prefer THP over DPC for large constellations.

### 3.1 Channel and pathloss model

A standard path loss propagation model is used with path loss exponent  $\alpha$  propagation model for urban areas. Specifically, we use the non-LOS (Line of Sight) pathloss model specified by ITU (International Telecommunication Union) for urban users. Assuming omnidirectional antennas with unit gain at both transmitter and receiver, the loss (in dB) between the transmitter and receiver separated at a distance  $r$  is given by

$$L(\text{dB}) = 10\alpha \log r + 22.7 + 26.0 \log f_c \quad (3.1)$$

where  $f_c$  denotes the carrier frequency and  $\alpha = 3.7$ . In linear scale, this can be written as

$$P_R/P_T = r^{-\alpha}/K \quad (3.2)$$

where  $K = 186.21f_c^{2.6}$ .

Independent Rayleigh fading with unit mean is assumed between any pair of BS and UE antennas. Therefore, the received signal voltage for a stream from  $BS_j$  to  $UE_i$  is given by  $\frac{1}{\sqrt{K}}h_{ij}r_{ij}^{-\alpha/2}$ , where  $r_{ij}$  is the distance between  $BS_j$  and  $UE_i$  and  $h_{ij}$  is the corresponding fading term with  $h_{ij} \in CN(0, 1)$ .

The noise term is assumed to be circularly symmetric complex Gaussian noise (AWGN) with zero mean and variance  $\sigma^2 = kTB$  where  $k$  is the Boltzmann constant,  $T$  is the temperature in Kelvin, and  $B$  is the operating bandwidth. The  $SNR = \frac{P_T r^{-\alpha}}{K\sigma^2}$  is defined to be the average received signal-to-noise-power ratio (SNR) for a user at a distance  $r$  from the BS.

### 3.2 Received signal vector

The cloud radio which is a collection of  $k$  BS selects  $k$  UEs i.e., one UE is chosen from a pool of active UEs associated with each BS (using round-robin strategy). The cloud radio transmits  $k$  distinct data streams. Assume  $k = 3$ . Hence, the received signal vector in downlink is given as:

$$y = Hx + n \quad (3.3)$$

where  $y = \begin{bmatrix} y_1 & y_2 & y_3 \end{bmatrix}'$  is the received signal vector,

$$H = \frac{1}{\sqrt{K}} \begin{bmatrix} h_{11}r_{11}^{-\alpha/2} & h_{12}r_{12}^{-\alpha/2} & h_{13}r_{13}^{-\alpha/2} \\ h_{21}r_{21}^{-\alpha/2} & h_{22}r_{22}^{-\alpha/2} & h_{23}r_{23}^{-\alpha/2} \\ h_{31}r_{31}^{-\alpha/2} & h_{32}r_{32}^{-\alpha/2} & h_{33}r_{33}^{-\alpha/2} \end{bmatrix}$$

where  $x = \begin{bmatrix} x_1 & x_2 & x_3 \end{bmatrix}'$  is the transmitted symbol vector with  $E[|x_i|^2] = P_T$  and  $n = \begin{bmatrix} n_1 & n_2 & n_3 \end{bmatrix}'$ , with  $n_i \in CN(0, 1)$  is AWGN. Expanding the equation 3.3 gives:

$$\begin{aligned} y_1 &= \frac{1}{\sqrt{K}}(h_{11}r_{11}^{-\alpha/2}x_1 + h_{12}r_{12}^{-\alpha/2}x_2 + h_{13}r_{13}^{-\alpha/2}x_3) + n_1; \\ y_2 &= \frac{1}{\sqrt{K}}(h_{21}r_{21}^{-\alpha/2}x_1 + h_{22}r_{22}^{-\alpha/2}x_2 + h_{23}r_{23}^{-\alpha/2}x_3) + n_2; \\ y_3 &= \frac{1}{\sqrt{K}}(h_{31}r_{31}^{-\alpha/2}x_1 + h_{32}r_{32}^{-\alpha/2}x_2 + h_{33}r_{33}^{-\alpha/2}x_3) + n_3; \end{aligned}$$

ie, Each UE's received signal consists of signals received from the all the BSs. For first user, signals received from BS2 and BS3 are considered as interferences. Similarly for other users also. Precoders are mainly designed to remove these interference effects.

### 3.3 THP Precoders

THP Precoder is basically a modification of ZF Precoder. It is a nonlinear preequalization technique that offers significant advantages over linear preequalization which increases average transmit power. Moreover, it outperforms decision-feedback equalization at the receiver side which is applicable if joint processing at the receiver side is possible, and which suffers from error propagation. By doing this one may incur a increased transmit signal power penalty [4]. So modulo operator at the transmitter and receiver is employed to limit the magnitude of the transmitted symbol and this

makes THP a non-linear scheme.

The THP structure consists of a feedback and feed-forward filter at the transmitter. The feedback filter cancels the interstream interference successively while the feed-forward filter ensures that the noise at the decision devices is spatially white [3]. The block diagram is shown in the figure 4.1

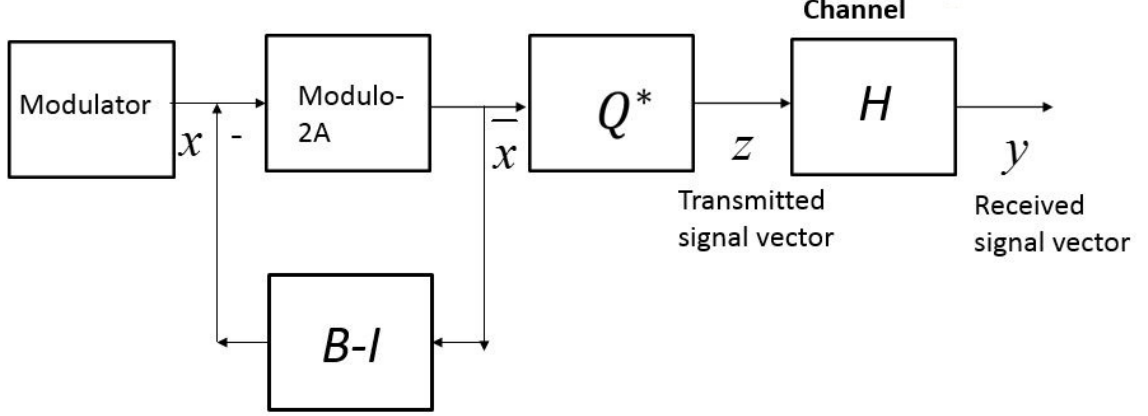


Figure 3.1: Transmitter schematic

### 3.3.1 Modulo Operation

Modulo Operation is used to limit the power of the transmitted signal. In THP Operation, we use modulo- $2A$  operation. It bounds the magnitude of the transmitted signal in  $[-A, A]$ .  $A$  is calculated as:

$$A = \left( \frac{M}{2*(M-1)} \right)^{1/2}$$

For QPSK,  $M=4$  and  $A=1.4$  For 16 QAM,  $M=16$ ,  $A=1.26$  For 64 QAM,  $M=64$ ,  $A=1.23$

The symmetric modulo operation is defined as:

$$\text{mod}_A(x) = x - 2A \left[ \frac{x}{2A} \right]$$

The above modulo operation can be interpreted as a method to find integer values,  $m$  and  $n$ , such that the following inequalities are satisfied:

$$-A - jA \leq \text{mod}_A(x) = x + 2Am + j2An \leq A + jA$$

### 3.3.2 Transmitter operation

The Channel matrix  $H$  is decomposed to  $L$  and  $Q$  matrices using  $LQ$  decomposition where  $L$  is a lower triangular matrix and  $Q$  is a Unitary matrix. Practically,  $QR$  decomposition of  $H^*$  is implemented.  $L$  and  $L$  values are derived from  $R^*$  and  $Q^*$ , where  $R$  is an upper triangular matrix. The  $QR$  decomposition always exists, even if the matrix does not have full rank, so the constructor will never fail. The primary use of the  $QR$  decomposition is in the least squares solution of non-square systems of simultaneous linear equations [1].

$$L = \begin{bmatrix} l_{11} & 0 & 0 \\ l_{21} & l_{22} & 0 \\ l_{31} & l_{32} & l_{33} \end{bmatrix}$$

$B$  in the feedback filter is defined like this:

$$B = L * S^{-1} \quad (3.4)$$

where  $S$  is adiagonal matrix whose diagonal entries same as that of  $L$  and  $S^{-1}$  is the inverse of  $S$ .  $S$  is defined as:

$$S = \begin{bmatrix} l_{11} & 0 & 0 \\ 0 & l_{22} & 0 \\ 0 & 0 & l_{33} \end{bmatrix}$$

and  $S^{-1}$  as

$$S^{-1} = \begin{bmatrix} 1/l_{11} & 0 & 0 \\ 0 & 1/l_{22} & 0 \\ 0 & 0 & 1/l_{33} \end{bmatrix}$$

$B$  is obtained as:

$$B = \begin{bmatrix} 1 & 0 & 0 \\ l_{21}/l_{22} & 1 & 0 \\ l_{31}/l_{33} & l_{32}/l_{33} & 1 \end{bmatrix}$$

ie,

$$\begin{aligned} B_{21} &= l_{21}/l_{22}; \\ B_{31} &= l_{31}/l_{33}; \\ B_{32} &= l_{32}/l_{33}; \end{aligned}$$

$B - I$  is a strictly lower triangular matrix,ie, diagonal elements have value as 0. From the schematic,

$$-(B - I)\bar{x} + x = \bar{x}$$

By expanding the equation, we get

$$\begin{aligned} \bar{x}_1 &= \text{mod}_{2A}(x_1); \\ \bar{x}_2 &= \text{mod}_{2A}(x_2 - B_{21}\bar{x}_1); \\ \bar{x}_3 &= \text{mod}_{2A}(x_3 - B_{31}\bar{x}_1 - B_{32}\bar{x}_2); \end{aligned}$$

From the block diagram, Transmitted vector  $z$  is:

$$z = Q^* * \bar{x}$$

Received vector  $y$  is:

$$\begin{aligned} y &= H * z + n \\ &= H * Q^* * Q^* * \bar{x} + n \\ &= L * \bar{x} + n \end{aligned}$$



Expanding it gives:

$$\begin{aligned} y_1 &= l_{11}\bar{x}_1 + n_1; \\ y_2 &= l_{21}\bar{x}_1 + l_{22}\bar{x}_2 + n_2; \\ y_3 &= l_{31}\bar{x}_1 + l_{32}\bar{x}_2 + l_{33}\bar{x}_3 + n_3; \end{aligned}$$

Using modulo values for  $\bar{x}$ , implies

$$\begin{aligned} y_1 &= l_{11} \text{mod}_{2A}(x_1) + n_1; \\ y_2 &= l_{21} \text{mod}_{2A}(x_1) + l_{22} \text{mod}_{2A}(x_2 - B_{21} \text{mod}_{2A}(x_1)) + n_2; \\ y_3 &= l_{31} \text{mod}_{2A}(x_1) + l_{32} \text{mod}_{2A}(x_2 - B_{21} \text{mod}_{2A}(x_1)) \\ &\quad + l_{33} \text{mod}_{2A}(x_3 - B_{31} \text{mod}_{2A}(x_1) - B_{32} \text{mod}_{2A}(x_2 - B_{21} \text{mod}_{2A}(x_1))) + n_3; \end{aligned}$$

By observing above equation, we can see that all other terms except the signals from the corresponding BS cancels out for each UE's received signal. Let modulo values be:

$$\begin{aligned} \text{mod}_{2A}(x_1) &= x_1 + 2Aa + j2Ab; \\ \text{mod}_{2A}(x_2) &= x_2 + 2Ac + j2Ad; \\ \text{mod}_{2A}(x_3) &= x_3 + 2Ae + j2Af; \end{aligned}$$

So the signals received by each UE is:

$$\begin{aligned} y_1 &= l_{11}(x_1 + 2Aa + j2Ab) + n_1; \\ y_2 &= l_{22}(x_2 + 2Ac + j2Ad) + n_2; \\ y_3 &= l_{33}(x_3 + 2Ae + j2Af) + n_3; \end{aligned}$$

Thus the received signals have become interference free.

### 3.3.3 Receiver operation

The receiver schematic for THP precoder is shown in the figure 3.2.

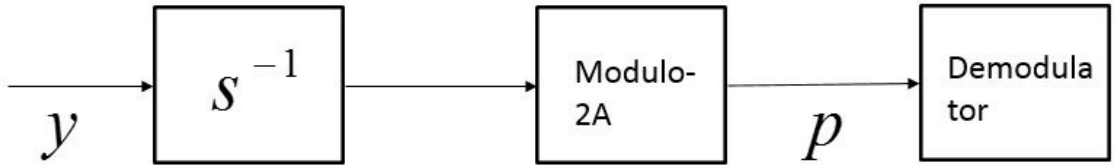


Figure 3.2: Receiver Schematic

$$\begin{bmatrix} p_1 \\ p_2 \\ p_3 \end{bmatrix} = \text{mod}_{2A} \left( S^{-1} \begin{bmatrix} y_1 \\ y_2 \\ y_3 \end{bmatrix} \right)$$

$$\begin{aligned}
&= \text{mod}_{2A} \left( \begin{bmatrix} 1/l_{11} & 0 & 0 \\ 0 & 1/l_{22} & 0 \\ 0 & 0 & 1/l_{33} \end{bmatrix} \begin{bmatrix} l_{11}(x_1 + 2Aa + j2Ab) + n_1 \\ l_{22}(x_2 + 2Ac + j2Ad) + n_2 \\ l_{33}(x_3 + 2Ae + j2Af) + n_3 \end{bmatrix} \right) \\
&= \begin{bmatrix} x_1 \\ x_2 \\ x_3 \end{bmatrix} + \begin{bmatrix} \bar{n}_1 \\ \bar{n}_2 \\ \bar{n}_3 \end{bmatrix}
\end{aligned}$$

where effective noise at the receiver  $\bar{n}$  is given by:

$$\begin{bmatrix} \bar{n}_1 \\ \bar{n}_2 \\ \bar{n}_3 \end{bmatrix} = \begin{bmatrix} \frac{n_1}{l_{11}} + 2Aa1 + j2Ab1 \\ \frac{n_2}{l_{22}} + 2Ac1 + j2Ad1 \\ \frac{n_3}{l_{33}} + 2Ae1 + j2Af1 \end{bmatrix}$$

It is obvious from the equation that the noise at the receiver is scaled down by a factor corresponding to the channel characteristics. The demodulator input in the transmitter is same as that of modulator output at the receiver . ie, it ensures reliable communication in the cloud network.

### 3.4 THP implementation for 6x6 cloud

The BS and UE distribution follows Poisson point process (PPP). In our proposed model, we assumed 6 BS and 6 UE in a particular area. ie, it forms 6x6 cloud. Each BS is associated with a UE. Each BS transmits an OFDM subframe to the UE associated with it. We revised the pilot positions in the ofdm subframe and are shown in figures 4.1, 4.2 and 4.3. In a subframe, data is transmitted expect in the first two ofdm symbols. Data in each resource element is modulated first and then THP precoded. The pilots and nulls are neither modulated nor precoded. When a BS transmits pilot, other BSs transmit nulls. They are transmitted as such and are used for channel estimation, which is explained in the next chapter. We will deal about the real time implementation of THP in the coming chapters.

#### 3.4.1 Psuedo code for THP implementation in Matlab

The psuedo code for THP implementation in matlab is given below:

```

EbNo ← [0:5:20];
for all reads ii do
  SNR ← EbNo(ii)
  std ← 10^(-SNR/20)
  Generate inf bits 0 or 1 randomly for each BS
  do modulation for the data bits transmitted by each BS (either QAM,
    16QAM and 64QAM) to generate x
  Generate channel matrix H which follows Rayleigh distribution
  Find L and Q matrices by using LQ decomposition of H
  Find S and inv(S)
  Find B matrix values by multiplying L with inv(S)
  Find transmitted signal x1 by solving the equation mod (x-(B-I)*x1)=x1
    where mod implies modulo operation for
      the signal from each BS
  Premultiply the signal x1 with Q*
  Find received signal whose value is H*Q**x1 and noise added to it
  Pre-multiply the received signal with inv(S)
  do modulo operation for the received signal for each UE
  do demodulation
  Calculate ber for each iteration
end for

```

# Chapter 4

## Channel Estimation

Channel estimation is used for coherent detection of received signal. In order to estimate the channel, LTE systems use pilot signals called reference signals. A Reference Signal (RS) is a pre-defined signal, pre-known to both transmitter and receiver. They are being transmitted during the first and second OFDM symbols as per our modified architecture as shown in figures 4.1, 4.2 and 4.3. They are different for each BS. We use Walsh matrix for pilots. Walsh matrix is a specific square matrix with dimensions of some power of 2, entries of 1 or  $-1$ , and the property that the dot product of any two distinct rows (or columns) is zero. In our case, we need a  $2 \times 2$  Walsh matrix.

The subframe structure for the BSs in our proposed model is shown in figures 4.1, 4.2 and 4.3.

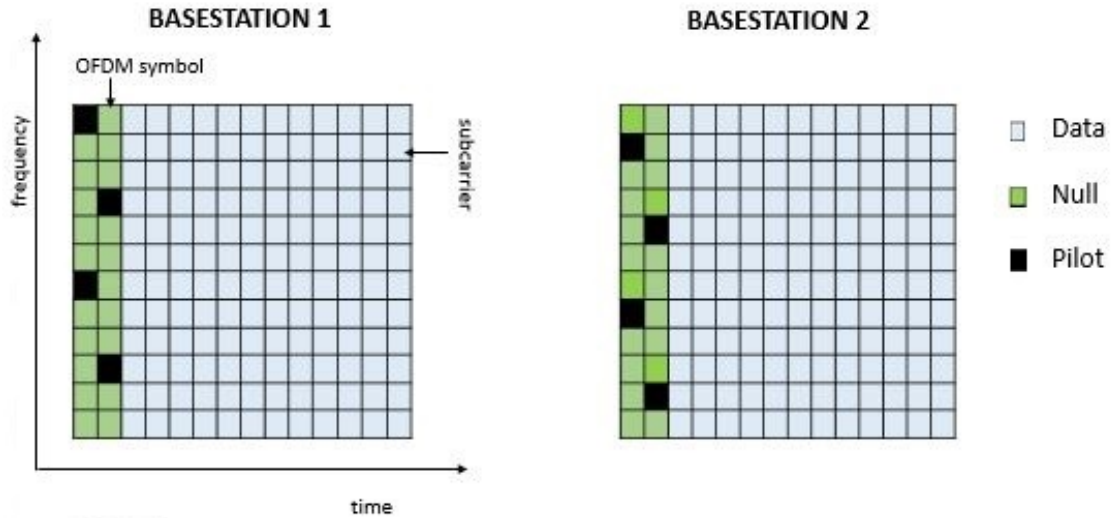


Figure 4.1: Subframe structure for BS 1 and BS 2

The received pilot signals can be written as:

$$Y_P = X_P H_P + N_P \quad (4.1)$$

where  $(.)_P$  denotes positions where reference signals are transmitted. We implemented Least Square (LS) channel estimation technique.

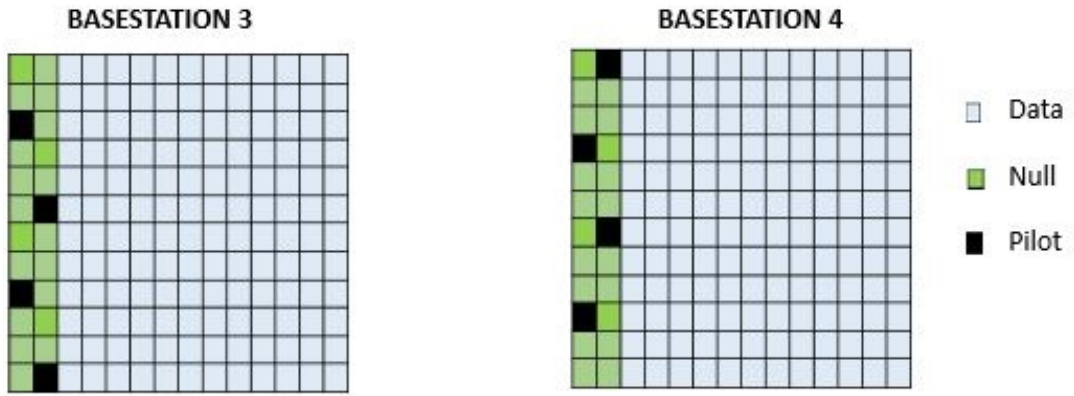


Figure 4.2: Subframe structure for BS 3 and BS 4

## 4.1 Least Square (LS)

The goal of the channel least square estimator is to minimize the square distance between the received signal and the original signal. The least square estimate (LS) of the channel at the pilot subcarriers given in equation 4.1 can be obtained by the following equation 4.2:

$$H_P^{LS} = (X_P)^{-1}Y_P \quad (4.2)$$

where  $H_P^{LS}$  represents the least-squares (LS) estimate obtained over the pilot subcarriers.

Channel is assumed to be the same for 3 consecutive subcarriers as shown in the figure 4.4. So,

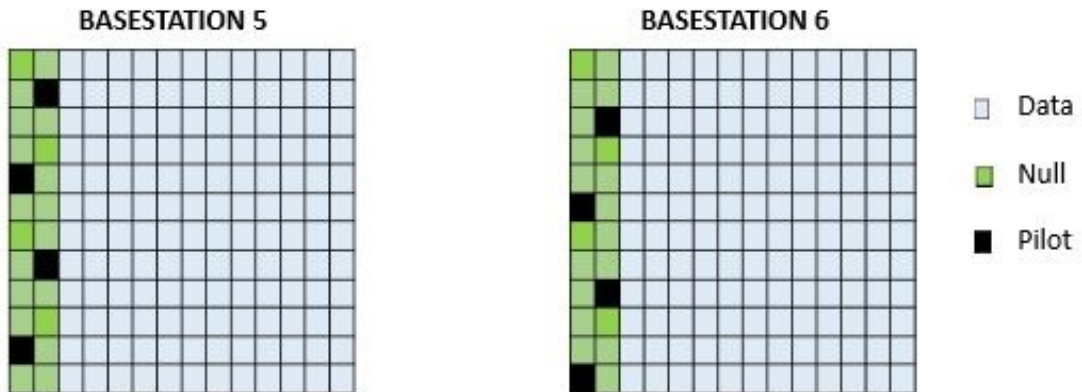


Figure 4.3: Subframe structure for BS 5 and BS 6

4 channels are associated with a resource block since 12 subcarriers come under one resource block. Let  $y_1, y_2, y_3, y_4, y_5$  and  $y_6$  be the symbols (resource block) received by each user and  $x$  denotes

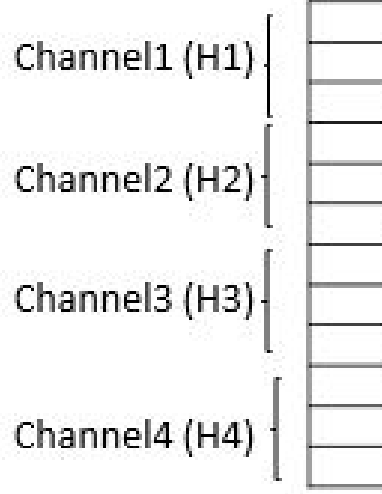


Figure 4.4: Different channels in a resource block

pilot symbol which can take values 1 or  $-1$ .

Let  $H_1$  be the channel matrix corresponding to first 3 subcarriers. The channel from first UE to first BS is found by extracting the 11 th element of  $y_1$  and dividing it with the pilot symbol value in that position. The channel from first UE to second BS is found by extracting the 21 th element of  $y_1$  and dividing it with the pilot symbol value in that position. The channel from first UE to third BS is found by extracting the 31 th element of  $y_1$  and dividing it with the pilot symbol value in that position. The channel from first UE to fourth BS is found by extracting the 132 th element of  $y_1$  and dividing it with the pilot symbol value in that position. The channel from first UE to fifth BS is found by extracting the 22 th element of  $y_1$  and dividing it with the pilot symbol value in that position. The channel from first UE to sixth BS is found by extracting the 32 th element of  $y_1$  and dividing it with the pilot symbol value in that position.  $H_1$  is given by :

$$H_1 = \begin{bmatrix} \left(\frac{y_1}{x}\right)_{11} & \left(\frac{y_1}{x}\right)_{21} & \left(\frac{y_1}{x}\right)_{31} & \left(\frac{y_1}{x}\right)_{12} & \left(\frac{y_1}{x}\right)_{22} & \left(\frac{y_1}{x}\right)_{32} \\ \left(\frac{y_2}{x}\right)_{11} & \left(\frac{y_2}{x}\right)_{21} & \left(\frac{y_2}{x}\right)_{31} & \left(\frac{y_2}{x}\right)_{12} & \left(\frac{y_2}{x}\right)_{22} & \left(\frac{y_2}{x}\right)_{32} \\ \left(\frac{y_3}{x}\right)_{11} & \left(\frac{y_3}{x}\right)_{21} & \left(\frac{y_3}{x}\right)_{31} & \left(\frac{y_3}{x}\right)_{12} & \left(\frac{y_3}{x}\right)_{22} & \left(\frac{y_3}{x}\right)_{32} \\ \left(\frac{y_4}{x}\right)_{11} & \left(\frac{y_4}{x}\right)_{21} & \left(\frac{y_4}{x}\right)_{31} & \left(\frac{y_4}{x}\right)_{12} & \left(\frac{y_4}{x}\right)_{22} & \left(\frac{y_4}{x}\right)_{32} \\ \left(\frac{y_5}{x}\right)_{11} & \left(\frac{y_5}{x}\right)_{21} & \left(\frac{y_5}{x}\right)_{31} & \left(\frac{y_5}{x}\right)_{12} & \left(\frac{y_5}{x}\right)_{22} & \left(\frac{y_5}{x}\right)_{32} \\ \left(\frac{y_6}{x}\right)_{11} & \left(\frac{y_6}{x}\right)_{21} & \left(\frac{y_6}{x}\right)_{31} & \left(\frac{y_6}{x}\right)_{12} & \left(\frac{y_6}{x}\right)_{22} & \left(\frac{y_6}{x}\right)_{32} \end{bmatrix}$$

Similarly,  $H_2, H_3,$  and  $H_4$  can be calculated. The estimated channel coefficients are feedback to the cloud using uplink

## Chapter 5

# Simulation Results

We have simulated a cloud radio network with THP encoding using PPP framework. We assumed a 3x3 cloud and the simulations were done in MATLAB. We simulated the Bit-error-rate performance of THP precoded system by adding a controlled amount of noise to the transmitted signal and assumed a flat fading Rayleigh channel in between BSs and UEs. BER vs SNR diagram is plotted in figure 5.1 for QPSK, 16 QAM and 64 QAM. As the SNR value is increased, the BER value is considerably reduced. Thus ensures error free communication. We can see that THP in QPSK performs better than 16 QAM and 64 QAM similar to the system without THP.

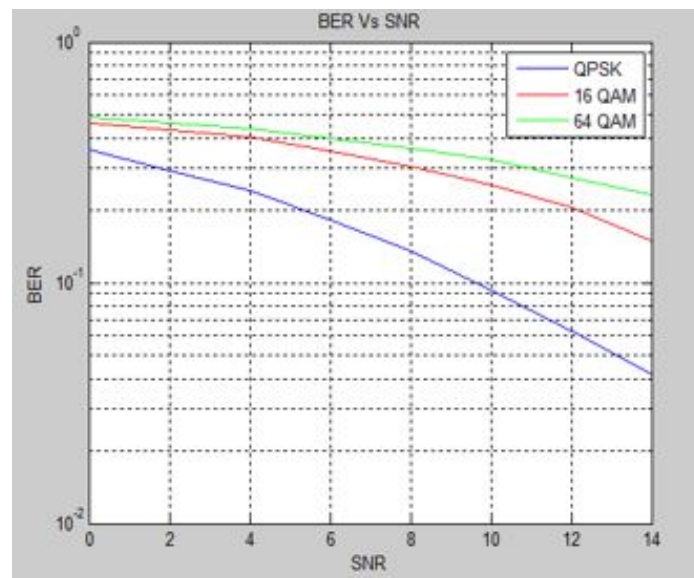


Figure 5.1: BER VS SNR plot

## Chapter 6

# CRAN prototype implementation

For real time implementation of CRAN, CCS studio is the software used for the dsp processors in the LTE testbed. Code Composer Studio is an integrated development environment (IDE) that supports TI's Microcontroller and Embedded Processors portfolio. Code Composer Studio comprises a suite of tools used to develop and debug embedded applications. It includes an optimizing C/C++ compiler, source code editor, project build environment, debugger, profiler, and many other features. The intuitive IDE provides a single user interface taking you through each step of the application development flow. Familiar tools and interfaces allow users to get started faster than ever before. Code Composer Studio combines the advantages of the Eclipse software framework with advanced embedded debug capabilities from TI resulting in a compelling feature-rich development environment for embedded developers.

As of now, we completed THP precoding for transmitter frames in CCS studio and working on channel estimation and processing of receiver frames. The figure 6.1 shows the performance improvement for THP precoding of a resource element and LQ decomposition of the particular channel using different optimization schemes in CCS studio. After completing the codes in CCS studio, we are planning to test the validity for real time implementation in Tejas networks' LTE testbed.

<b>Optimization items</b>	<b>DSP cycle count in CCS studio</b>	<b>Time in microseconds</b>
Original floating point	90, 842	90
SIMD formats	40, 562	40
Using optimization level 3 in CCS	11, 341	11

Figure 6.1: Table showing performance improvement for THP precoding of a resource element and LQ decomposition of the particular channel using different optimization schemes in CCS studio



## 6.1 LTE Testbed

The figure 6.2 lte shows the LTE Testbed. RRHs, setup containing eDC cards, Gigabit Ethernet switch and PC used for working on CCS studio is also marked in the 6.2 Our setup consists of 6 BSs

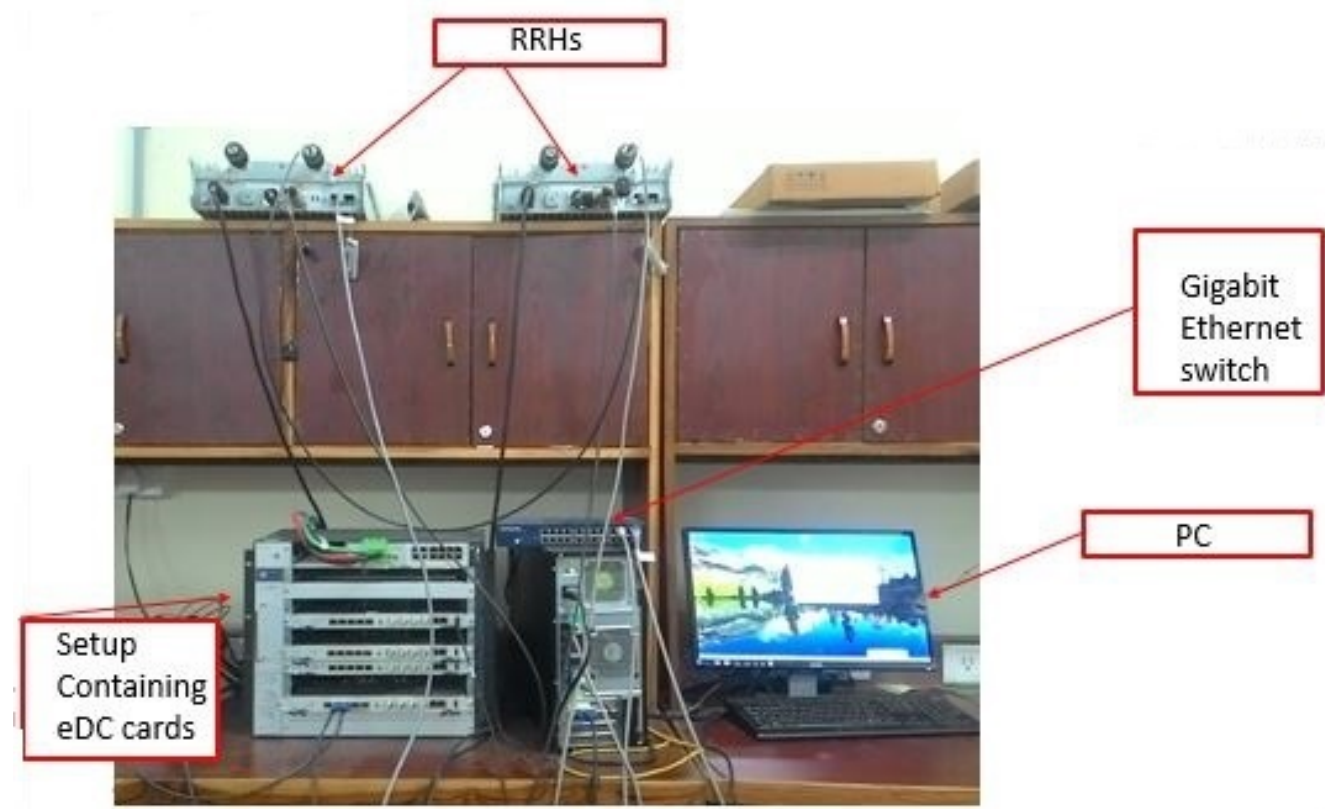


Figure 6.2: LTE Testbed

and 6 UEs. The architecture of LTE test bed is described below:

### 6.1.1 Hardware

Each eDC card contain 3 DSPs which can handle 3 sectors of a base station But in our case we use each DSP to handle one base station. So 2 eDCs are used for implementing the 6 BSs and 2 eDCs for 6UEs.

Each DSP is connected to RRH through optical fiber. Each DSP has 4 computing cores and extra hardware for FFT and Turbo encode and decode. CORE 0 is configured for DL Tx and CORE 1 for UL Rx as the RRHs are TDD and can be used with BAND 40 spectrum. CORE 2 and CORE 3 are used to perform extra signal processing operations at peak loads.

### 6.1.2 Cloud Implementation

THP is implemented on CORE 0 of the BS DSPs and CORE 2 and 3 can be leveraged to speed up the operations. The UEs are configured to receive only mode and CORE 1 is used to receive the

IQ samples. CORE 0, 1, 2 and 3 can be used to implement the THP receiver algorithms. There is no UL so the ACKS and CSI are feed back using the Ethernet back-haul network.

First we need to boot linux in each eDC card separately. For this we have a script which has to be executed using TeraTerm. After booting the linux in each card, we need to setup telnet sessions with each card using TeraTerm. Each card is assigned a static IP. Before starting the telnet sessions, we need to ensure that the PC also has a IP assigned to it in the same domain. Next task is to boot all the cores of all DSPs in the setup. After this we need to communicate to each board about its own configuration and the configuration of the other boards i.e. whether UE or eNodeB.

# References

- [1] Windpassinger, Christoph, Robert FH Fischer, Tom Vencel, and Johannes B. Huber. “Precoding in multiantenna and multiuser communications”, *Wireless Communications, IEEE Transactions on* 3, no. 4 (2004): 1305-1316.
- [2] Akoum, S., Heath, R.W., “Interference Coordination: Random Clustering and Adaptive Limited Feedback”, *IEEE Transactions on Signal Processing*, vol.61, no.7, pp.1822,1834, April. 2013
- [3] Sharma, D., Kizhakkemadam, S.N., “Cascaded tomlinson harshima precoding and block diagonalization for multi-user MIMO”, *National Conference on Communications (NCC), 2011*, vol., no., pp.1,5, 28-30 Jan. 2011
- [4] Robert F.H.Fischer, Christoph Windpassinger, Alexander Lampe, and Johannes B.Huber, “Space-time transmission using Tomlinson-Harshima precoding”, *International ITG Conference on Source and Channel Coding*, pp.139-147, 2002
- [5] Kuchi, K., Mohiuddin, M.M., Sreejith, T.V., Bansal, R., Sharma, G.V.V., Emami, S., “Cloud radios with limited feedback”, *Signal Processing and Communications (SPCOM), 2014 International Conference on* , vol., no., pp.1,6, 22-25 July 2014